SUPPORTING INFORMATION FOR

Emergence of Novel Polynitrogen Molecule-Like Species, Covalent Chains and Layers in Magnesium-Nitrogen Mg_xN_y Phases under High Pressure

Shuyin Yu,[†,‡] Bowen Huang,[§] Qingfeng Zeng,[†,‡] Artem R. Oganov,[∥,†,⊥,#] Litong Zhang, [†] and Gilles Frapper[*,§]

[†] *Science and Technology on Thermostructural Composite Materials Laboratory, School of Materials Science and Engineering, Northwestern Polytechnical University, Xi'an, Shaanxi 710072, China*

[‡] *International Center for Materials Discovery, School of Materials Science and Engineering, Northwestern Polytechnical University, Xi'an, Shaanxi 710072, China*

[§] *IC2MP UMR 7285, Université de Poitiers - CNRS, 4, rue Michel Brunet TSA 51106 - 86073 Poitiers Cedex 9, France*

[∥] *Skolkovo Institute of Science and Technology, 3 Nobel Street, Moscow 143026, Russia*

[⊥] *Department of Geosciences, Center for Materials by Design, and Institute for Advanced Computational Science, State University of New York, Stony Brook, NY 11794-2100, USA*

[#] *Moscow Institute of Physics and Technology, Dolgoprudny, Moscow Region 141700, Russia*

**Corresponding author: gilles.frapper@univ-poitiers.fr*

Table S1 Structural parameters of the predicted Mg_xN_y compounds at selected pressures (distances in Å, angles in °, pressure in GPa)

Phase	Z	P	Lattice parameters	Atomic coordinates (fractional)	Bond length	
					N-N	Mg-N
Stable compounds						
Mg_5N_3 *$P6_3/mcm$*	2	150	a=5.472, c=4.246	Mg (0, 0.749, 0.75) (0.333, 0.667, 1); N (0, 0.388, 0.75)	>2	1.865~2.002
Mg_3N_2 *Ia-3*	16	0	a=9.992 Exp[1]: a=9.936(7)	Mg (0.118, 0.389, 0.847); N (0.25, 0.25, 0.75) (0.031, 0.5, 0.25)	>2	2.095~2.192
Mg_3N_2 *Pbcn*	4	30	a=7.353, b=5.141 c=5.242	Mg (0.152, 0.106, 0.607) (0, 0.547, 0.750); N (0.615, 0.753, 0.532)	>2	1.989~2.133
Mg_3N_2 *C2/m*	6	50	a=11.931, b=3.074, c=7.485, β=99.1 Exp[1]: (32.5 GPa) a=12.229, b=3.157 c=7.618, β=99.03	Mg (0.130, 0.5, 0.288) (0.797, 0.5, 0.369) (0.828, 0.5, 0.03) (0.971, 0, 0.34) (0, 0, 0) N (0.033, 0.5, 0.814) (0.863, 0, 0.515) (0.815, 0, 0.863)	>2	1.871~2.282
Mg_3N_2 *Pnma*	4	40	a=5.280, b=2.967 c=11.427	Mg (0.361, 0.250, 0.561) (0.525, 0.250, 0.106) (0.636, 0.250, 0.718); N (0.168, 0.250, 0.197) (0.238, 0.750, 0.452)	>2	1.975~2.381
Mg_4N_3 *I-43d*	4	100	a=5.873	Mg (0.321, 0.179, 0.821) N (0.625, 0, 0.75)	>2	1.957~2.114
Mg_5N_4 *Cmca*	4	200	a=9.487, b=4.793 c=4.811	Mg (0.147, 0.324, 0.671) (0, 0.5, 1) N (0, 0.11, 0.889) (0.2, 0.5, 1)	1.501	1.828~2.024
Mg_5N_7 *C2*	2	250	a=5.67, b=4.517 c=5.005, β=98.6	Mg (0.739, 0, 0.213) (0.323, 0.502, 0.79) (0, 0.363, 0.5);N (0.561, 0.22, 0.906) (0.812, 0.731, 0.501) (0.556, 0.785, 0.894) (0, 0.917, 0.5)	1.248/1.316 /1.358	1.829~2.069
Mg_2N_3 *Pmmn*	2	50	a=9.104,b=2.728 c=3.071	Mg (0.147, 0, 0.726) N (0.868, 0.5, 0.213) (0, 0.5, 0.428)	1.371	2.021~2.118
MgN_2 *Cmcm*	4	40	a=3.805,b=7.777,c=3.192	Mg (0, 0.363, 0.75) N (0.664, 0.603, 0.75)	1.248	2.062~2.262
MgN_2 *$P6_3/mcm$*	4	100	a=4.387, c=4.782	Mg (0.667, 0.333, 0) N (0, 0, 0.25) (0, 0.292, 0.25)	1.281	1.964~1.968
MgN_3 *P-1 (II)*	2	200	a=3.574, b=3.551 c=3.598, α=101 β=69.4, γ=105	Mg (0.122, 0.824, 0.135); N (0.335, 0.373, 0.11) (0.314, 0.515, 0.487) (0.306, 0.895, 0.58)	1.332~1.397	1.887~1.972
MgN_3 *P-1 (I)*	2	50	a=4.866, b=4.830 c=2.768, α=78.7 β=78.7, γ=61.2	Mg (0.667, 0.671, 0.478) N (0.796, 0.306, 0.054) (0.692, 0.106, 0.981) (0.903, 0.814, 0.856)	1.344~1.350	2.058~2.468
MgN_4 *Cmmm*	2	100	a=3.521, b=7.312 c=2.393	Mg (0.667, 0, 0) N (0.684, 0.166, 0.5)	1.296~1.313	2.035
MgN_4 *P-1*	1	10	a=3.059, b=3.812 c=4.075, α=101.7 β=86.2, γ=69.4	Mg (0, 0,0.5); N (0.578, 0.516, 0.852) (0.443, 0.126, 0.159)	1.311~1.390	2.102~2.250

Meta-stable compounds						
Mg_5N_3 *Cmcm*	4	0	a=4.113, b=10.414, c=10.558	Mg (1, 0.191, 0.575) (1, 0.259, 0.25) (1, 0.548, 0.116); N (1, 0.306, 0.75) (1, 0.356, 0.437)	> 2	2.076~2.253
Mg_3N_2 *P-3m1*	1	100	a=3.14, c=4.528 Exp[1]: (70 GPa) a=3.177, c=4.784	Mg (0.333, 0.667, 0.665) (0, 0, 0) N (0.333, 0.667, 0.227)	>2	1.876~2.085
Mg_4N_3 *C2*	4	0	a=9.937, b=5.502 c=13.599, β=154.1	Mg (0, 0.162, 1) (0.115, 0.314, 0.861) (0.266, 0.105, 0.773) (0.360, 0.265, 0.605) (0, 0.6, 0.5); N (0.254, 0.958, 0.917) (0.105, 0.454, 0.704) (0.148, 0.952, 0.556)	1.706	2.055~2.355
Mg_5N_4 *R3m*	3	0	a=3.420 c=31.208	Mg (0, 0, 0.611) (0, 0, 0.340) (0, 0, 0.477) (0, 0, 0.076) (0, 0, 0.881); N (0, 0, 0.541) (0, 0, 0.970) (0, 0, 0.778) (0, 0, 0.721)	1.779	1.985~2.472
Mg_5N_7 *Imm2*	2	0	a=22.821 b=3.389, c=4.133	Mg (0.132, 0.5, 0.199) (0.558, 0.5, 0.210) (0.5, 0, 0.711); N (0.218, 0.5, 0.561) (0.190, 0.5, 0.790) (0.414, 0.5, 0.712) (0.5, 0, 0.211)	1.142	1.994~2.468
Mg_2N_3 *C2/m*	2	0	a=5.631, b=3.131 c=7.310, β=113.7	Mg (0.089, 0.5, 0.846); N (0.956, 0, 0.412) (0.5, 0.5, 0)	1.178	2.103~2.385
MgN_2 *Cm*	4	0	a=5.686, b=3.274 c=10.026, β=128.2	Mg (0.735, 0, 0.442) (0.180, 0.5, 0.699); N (0.465, 0.5, 0.965) (0.220, 0, 0.582) (0.186, 0, 0.257) (0.071, 0, 0.109)	1.171/1.196	2.096~2.454
MgN_3 *C2/m*	4	0	a=9.285, b=3.104 c=6.229, β=100.3	Mg (0.379, 0.5, 0.755); N (0.282, 0.5, 0.212) (0.382, 0.5, 0.116) (0.451, 0, 0.551)	1.191/1.199	2.185~2.244
MgN_4 *P2/m*	1	0	a=5.484, b=3.097 c=4.199, β=94.4	Mg (0, 0, 0); N (0.999, 0.5, 0.644) (0.397, 0, 0.014)	1.142/1.210	2.152~2.175
MgN_4 *C2/c*	4	205	a=5.912, b=3.678 c=4.697, β=97.6	Mg (0, 0.047, 0.75); N (0.079, 0.597, 0.956) (0.246, 0.392, 0.914)	1.280~1.320	1.863~2.041

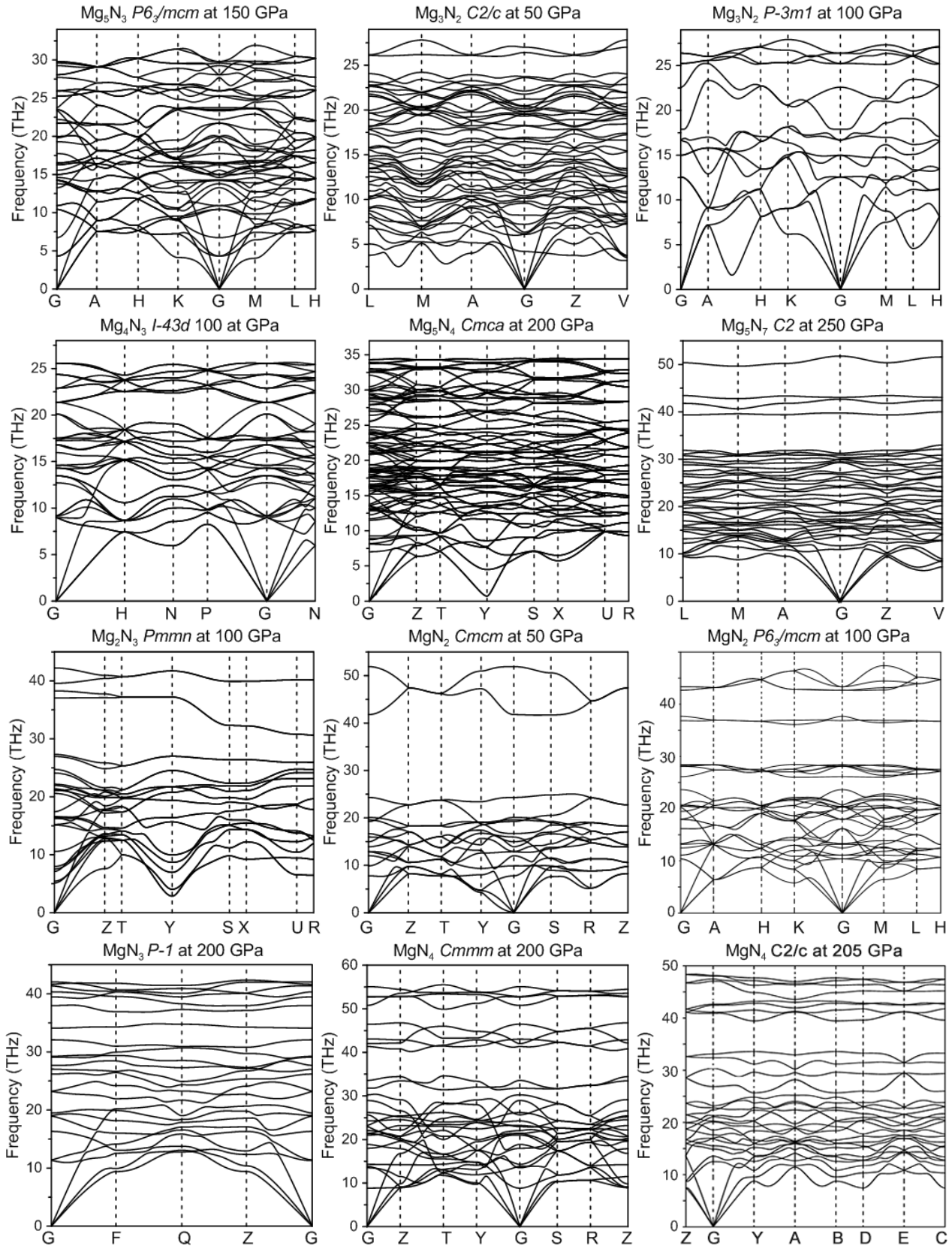

Figure S1 Phonon dispersion curves of the Mg_xN_y compounds at selected pressures. No imaginary phonon modes are found in the whole Brillouin zone, which confirms their dynamical stability.

Table S2 The calculated zero point energy (ZPE, eV/atom) of the Mg_xN_y compounds at selected pressures (P, GPa)

Phase	P	ZPE	Phase	P	ZPE	Phase	P	ZPE
Mg *P6$_3$/mmc*	0	0.032	Mg_5N_3 *P6$_3$/mcm*	100	0.101	Mg_4N_3 *I-43d*	100	0.102
	25	0.050		200	0.114		200	0.126
	50	0.060		300	0.141		300	0.143
Mg *Im-3m*	100	0.072	Mg_5N_4 *Cmca*	50	0.081	Mg_5N_7 *C2*	250	0.144
	200	0.088		200	0.131		270	0.148
	300	0.097		300	0.148		290	0.151
Mg_3N_2 *Ia-3*	0	0.070	Mg_2N_3 *Pmmn*	50	0.104	MgN_3 *P-1*	150	0.151
	10	0.078		80	0.115		200	0.162
	20	0.087		100	0.122		300	0.179
Mg_3N_2 *C2/m*	30	0.085	MgN_2 *Cmcm*	35	0.105	MgN_4 *Cmmm*	50	0.131
	50	0.090		40	0.107		100	0.146
	60	0.097		45	0.109		200	0.173
Mg_3N_2 *P-3m1*	70	0.099	MgN_2 *P6$_3$/mcm*	50	0.120	MgN_4 *C2/c*	205	0.162
	80	0.103		80	0.130		207	0.162
	100	0.108		100	0.136		209	0.162
N_2 *Pa-3*	0	0.083	N_2 *Pba2*	150	0.179	N_2 *I-43m*	150	0.186
N_2 *P4$_1$2$_1$2*	30	0.119		200	0.190		200	0.195
N_2 *I2$_1$3*	100	0.175		250	0.199		250	0.203
	150	0.186		300	0.207		300	0.210

Table S3 Literature report on A_xN_y binary phases (A, s-block elements; alkaline and alkaline earth metals). These structures are classified into four families related the dimensionality of the nitrogen sublattices: (1) extended 2D nitrogen layers, (2) infinite 1D nitrogen chains, (3) encapsulated molecule-like 0D anionic units, and (4) isolated nuclei N^{3-} ions.

Phases	P (GPa)	VEC[a]/ACN[b]	Nitrogen framework, electrical property
Two-dimensional (2D) network			
LiN_3 (*C2/m*) Prasad[2]	190-500	5.33/2.6+2	layers of fused puckered 10-embered decagon rings + 1D zigzag chains, metallic
MgN_3 (*P-1*) This work	115-300	5.67/2.33	fused puckered 14-membered rings, insulator
One-dimensional (1D) network			
LiN_2 (*P-1*) Shen[3]	>56	5.5/2	polyacetylene-like armchair chains poly-N_4^{2-}, semiconductor
LiN_3 (*P-1*) Prasad[2]	metastable	5.33/2.33	linked chair six-membered rings poly-N_6^{2-}, metallic
LiN_3 (*P2$_1$*) Wang[4]	>375	5.33/2.67	puckered fused 5-membered rings poly-N_6^{2-}, insulator
NaN_2 (*Cmmm*) Steele[5]	50-100	5.5/2	polyacetylene-like zigzag chains poly-N_2^{-}, metallic
NaN_3 (*C2/m*) Zhang[6]	152-200	5.33/2.5+2	puckered fused six-membered rings poly-N_4^{-} and zigzag chains poly-N_2^{-}, metallic
KN_3 (*P6/mmm*) Zhang[7]	40-100	5.33/2.67	Fused chair-like six-membered rings poly-N_6^{2-}, metallic
KN_3 (*C2/m*) Li[8]	>298.6	5.33/2.5+2	puckered fused six-membered rings poly-N_4^{-} and zigzag chains poly-N_2^{-}, metallic
KN_3 (*C2/m*) Zhang[9]	>274	5.33/2.67	Fused chair-like six-membered rings poly-N_6^{2-}, insulator
RbN_3 (*P-1*) Wang[10]	30-50	5.33/2	polyacetylene-like trans-cis chains poly-N_{12}^{4-} , metallic
RbN_3 (*C2/m*) Wang[10]	>200	5.33/2.67	Fused chair-like six-membered rings poly-N_6^{2-}, metallic
CsN_3 (*P-1*) Wang[11]	51-200	5.33/2	polyacetylene-like trans-cis chains poly-N_{12}^{4-}, metallic
CsN_2 (*C2/c*) Peng[12]	>40	5.5/2	infinite spiral chains poly-N_8^{4-}, insulator
MgN_4 (*Cmmm*) This work	14-199	5.67/2	polyacetylene-like armchair chains poly-N_4^{2-}, metallic
CaN_4 (*P4$_1$2$_1$2*) Zhu[13]	19-67	5.5/2	armchair chains poly-N_4^{2-}, metallic
Molecular anions			
Li_3N_2 (*P4/mbm*) Shen[3]	30-39	6.5/1	dumbbell N_2^{3-}, metallic
Li_3N_2 (*C2/c*) Shen[3]	39-89	6.5/1	dumbbell N_2^{3-}, metallic
Li_2N_2 (*Pmmm*)	0-8.2	6/1	dumbbell N_2^{2-}, metallic

Shen[3], Zhang[14]			
Li_2N_2 (*Immm*) Shen[3]	8.2-8.9	6/1	dumbbell N_2^{2-}, metallic
Li_2N_2 (*Pnma*) Shen[3]	8.9-66.4	6/1	dumbbell N_2^{2-}, metallic
Li_2N_2 (*Cmcm*) Shen[3]	>66.4	6/1	dumbbell N_2^{2-}, metallic
Li_2N_2 ($P6_3/mmc$) Shen[3]	0-56	5.5/1	dumbbell N_2^{2-}, metallic
LiN_3 (*P-62m*) Shen[3]	0-0.9	5.33/1	dumbbells N_2^{-}, metastable
LiN_3 (*C2/m*) Vaitheeswaran[15]	0-36	5.33/1.33	linear N_3^- azide, metastable below 49 GPa (Shen[3])
LiN_3 (*P6/m*) Shen[3], Wang[4]	>49 36-375	5.33/2	benzene-like N_6^{2-}, metallic
KN_3 (*I4/mcm*) Zhang[7]	0-22	5.33/2	linear molecular N_3^- anions
KN_3 (*C2/m*) Zhang[7]	22-40	5.33/2.5+2	linear molecular N_3^- anions
LiN_5 ($P2_1/c$) Shen[3]	15-65	5.2/2	5-membered ring N_5^- pentazolate, insulator
LiN_5 (*C2/c*) Shen[3]	>65	5.2/2	5-membered ring N_5^- pentazolate, insulator
NaN (*Pmmm*) Zhang[14]	0	6/1	dumbells N_2^{2-}, metallic
NaN (*Cmcm*) Steele[5]	10-30	6/1	dumbells N_2^{2-}, metallic
NaN (*Cmmm*) Steele[5]	28-100	5.33/1	dumbells N_2^{2-}, metallic
NaN_2 (*Cmmm*) Steele[5]	30-100	5.5/1	dumbells N_2^{2-}, metallic
Na_2N_5 (*Pbam*) Steele[5]	30-100	5.4/1	Five-membered ring N_5^{2-}, pentazolate, metallic
NaN_3 (*C2/m*) Steele[5]	<0.85	5.33/1.33	linear N_3^- azide, insulator
NaN_3 (*R-3m*) Zhang[16]	0.85-6.5	5.33/1.33	linear N_3^- azide, insulator
NaN_3 (*I4/mcm*) Zhang[16]	6.5-58	5.33/1.33	linear N_3^- azide, insulator
NaN_3 (*P6/m*) Zhang[16]	58-152	5.33/2	benzene-like N_6^{2-}, metallic
NaN_5 (*P2/c*) Steele[5]	16.5	5.2/2	five-membered ring N_5^- pentazolate, insulator
NaN_5 (*Cm*) Steele[5]	20-100	5.2/2	five-membered ring N_5^- pentazolate, insulator
KN_3 (*I4/mcm*)	0-20	5.33/1.33	linear N_3^- azide insulator

Babu[15]			
KN_3 (*C2/m*) Zhang[7]	15.7-20	5.33/1.33	linear N_3^- azide, insulator
KN_3 ($Cm2_1$) Zhang[7]	20-41	5.33/1.33	linear N_3^-, azide; metastable
KN_3 (*P6/mmm*) Zhang[7]	>41	5.33/1.33	benzene-like N_6^{2-}, metallic
RbN_3 (*I4/mcm*) Wang[10]	0-30	5.33/1.33	linear N_3^- azide, insulator
RbN_3 (*P6/mmm*) Wang[10]	50-200	5.33/2	benzene-like N_6^{2-}, metallic
Cs_2N (*C2/m*) Peng[12]	>18	7/1	dumbbell N_2^{4-} pernitride
CsN (*C2/m*) Peng[12]	7.5-44	6/1	dumbbell N_2^{2-} diazenide
CsN (*P-1*) Peng[12]	>44	6/1	open-chain N_4^{4-} tetrazadiene, semiconductor
CsN_2 (*C2/m*) Peng[12]	4-40	5.5/1	dumbbell N_2^-
CsN_3 (*I4/mcm*) Peng[12]	<6	5.33/1.33	linear N_3^- azide, insulator
CsN_3 (*C2/m*) Peng[12]	6-13	5.33/1.33	linear N_3^- azide
CsN_3 ($P2_1/m$) Peng[12]	16-26	5.33/1.33	linear N_3^- azide
CsN_3 (*C2/m*) Peng[12]	>81	5.33/2	benzene-like N_6^{2-}, metallic
CsN_3 ($P2_1$) Wang[11]	13-51	5.33/1.33	linear N_3^- azide
CsN_5 ($Cmc2_1$) Peng[12]	>14	5.2/2	cyclopentadiene-like N_5^- pentazolate, metallic
MgN_2 (*Cmcm*) This work	30-44	6/1	dumbbell N_2
Mg_2N_3 (*Pmmn*) This work	41-133	6.33/1.33	bent N_3
MgN_2 ($P6_3/mcm$) This work	44-88	6/1.5	SO_3-like $N(N)_3^{4-}$
CaN (*C2/m*) Zhu[13]	0-14	7/1	dumbbell N_2, metallic
CaN ($Cmc2_1$) Zhu[13]	14-40	7/1	dumbbell N_2, metallic
CaN (*C2/m*) Zhu[13]	40-76	7/1	dumbbell N_2, metallic
CaN (*Pbam*) Zhu[13]	76-100	7/1	dumbbell N_2, metallic
Ca_2N_3 (*P-62m*)	18-44	6.33/	dumbbell N_2, metallic

Zhu[13]			
CaN_2 (*Pnma*) Zhu[13]	0-3	6/1	dumbbell N_2^{2-}
CaN_2 (*I4/mmm*) Zhu[13]	3-18	6/1	dumbbell N_2^{2-}
CaN_2 ($P2_1/c$) Zhu[13]	18-92	6/1.5	N_4^{4-}, metallic
CaN_2 (*Pbam*) Zhu[13]	92-100	6/1.5	N_4^{4-}, metallic
CaN_3 (*Pmma*) Zhu[13]	8-36	5.67/1	dumbbell N_2, metallic
CaN_4 (*P4/mbm*) Zhu[13]	5-19	5.5/1	dumbbell N_2, metallic
CaN_3 (*C2/c*) Zhu[13]	36-100	5.67/2	N_6^{4-}, metallic
CaN_5 (*Pm*) Zhu[13]	33-100	5.4/2	N_5^{2-}, metallic
CaN_6 (*Fddd*) Experiment	ambient	5.33/1.33	linear N_3^- azide
SrN_6 (*Fddd*) Zhu[17]	ambient	5.33/1.33	linear N_3^- azide, insulator
BaN_6 (*Fddd*) Zhu[18]	ambient	5.33/1.33	linear N_3^- azide, insulator
Isolated nitrides N^{3-}			
$Li_{13}N$ (*Immm*) Shen[3]	43-76	18/0	metallic
$Li_{13}N$ (*C2/m*) Shen[3]	>76	18/0	metallic
Li_5N (*P6/mmm*) Shen[3]	>80	10/0	metallic
Li_3N (*Pm-3m*) Shen[3]	0-0.2	8/0	insulator
Li_3N (*P6/mmm*) Shen[3]	0.2-	8/0	insulator
Li_3N ($P6_3/mmc$) Shen[3]	0.2-	8/0	insulator
Li_3N (*Fm-3m*) Shen[3]	0.2-	8/0	insulator
Na_3N (*Pm-3m*) Vajenine[19]	0-1	8/0	insulator
Na_3N (*P6/mmm*) Vajenine[19]	1-2.3	8/0	insulator
Na_3N ($P6_3cm$) Vajenine[19]	2.3-25	8/0	insulator
Na_3N ($P6_3cm$) Vajenine[19]	>25	8/0	insulator

Na_3N (*Fm-3m*) Steele[5]	>10	8/0	insulator
K_3N ($P6_3/mmc$) Fischer[20]	metastable	8/0	insulator
Cs_3N (*Cmcm*) Peng[12]	18-64	8/0	insulator
Be_3N_2 (*Ia-3*) Xia[21]	0-118	8/0	insulator
Be_3N_2 (*P-3m1*) Xia[21]	118-150	8/0	insulator
Be_3N_2 ($P6_3/mmc$) Xia[21]	metastable	8/0	insulator
Be_3N_2 (*Pn-3m*) Xia[21]	metastable	8/0	insulator
Be_3N_2 (*R3m*) Xia[21]	metastable	8/0	insulator
Mg_5N_4 (*Cmca*) This work	43-300	7.5/0	insulator
Mg_4N_3 (*I-43d*) This work	70-300	7.67/0	insulator
Mg_3N_2 (*Ia-3*) This work	0-23	8/0	insulator
Mg_3N_2 (*C2/m*) This work	23-63	8/0	insulator
Mg_3N_2 (*P-3m1*) This work	63-100	8/0	insulator
Mg_5N_3 ($P6_3/mcm$) This work	74-300	8.33/0	insulator
Ca_2N (*R-3m*) Zhu[13]	0-10	9/0	insulator
Ca_2N (*Fm-3m*) Zhu[13]	10-84	9/0	metallic
Ca_2N ($I4/mmm$) Zhu[13]	84-100	9/0	metallic
Ca_3N_2 (*Ia-3*) Römer[22]	0-0.5	8/0	insulator
Ca_3N_2 (*R-3c*) Römer[22]	metastable	8/0	insulator
Ca_3N_2 (*Pbcn*) Römer[22]	0.5-10	8/0	insulator
Ca_3N_2 (*C2/m*) Römer[22]	10-27	8/0	insulator
Ca_3N_2 (*P-3m1*) Römer[22]	27-38	8/0	insulator
Ca_3N_2 (*C2/m*) Römer[22]	38-90	8/0	insulator

[a]In A_xN_y, VEC is the valence electron concentration; VEC= (cx+5y)/y with c: number of electrons given by A; x: number of A atoms; y: number of nitrogen atoms.

[b]ACN is the averaged coordination number of the nitrogen atoms in A_xN_y structures.

Alkali metals, group 1	Alkaline earth metals, group 2
3 **Li** 1:1 stoichiometry Zhang[14] 1:3 stoichiometry Prasad[2], Wang[4] Complete phase diagram Shen[3]	4 **Be** 1:3 stoichiometry Xia[21]
11 **Na** 3:1 stoichiometry Vajenine[19, 23] 1:3 stoichiometry Zhang[14], Zhang[16] Complete phase diagram Steele[5]	12 **Mg** 3:2 stoichiometry Hao[24], Braun[25], Li[26] Complete phase diagram This work
19 **K** 3:1 stoichiometry Fischer[20] 1:3 stoichiometry Babu[15], Li[8], Zhang[7], Zhang[9]	29 **Ca** 3:2 stoichiometry Römer[22] Complete phase diagram Zhu[13]
37 **Rb** 1:3 stoichiometry Wang[10]	38 **Sr** 1:6 stoichiometry Zhu[18], Dong[27], Zhu[17]
55 **Cs** 1:3 stoichiometry Wang[11] Complete phase diagram Peng[12]	56 **Ba** 1:6 stoichiometry Zhu[18]

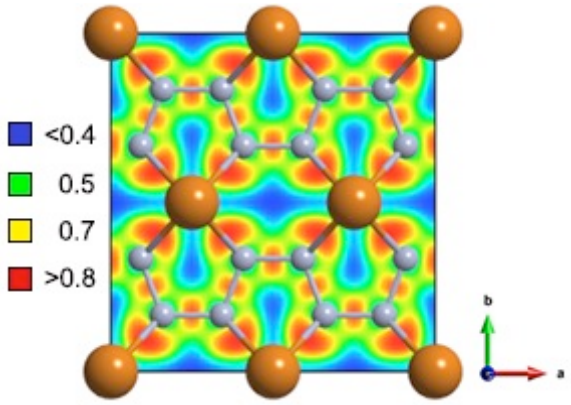

Figure S2 The calculated electron localization function (ELF) of the (001) plane of *Cmmm* MgN_4 at 100 GPa.

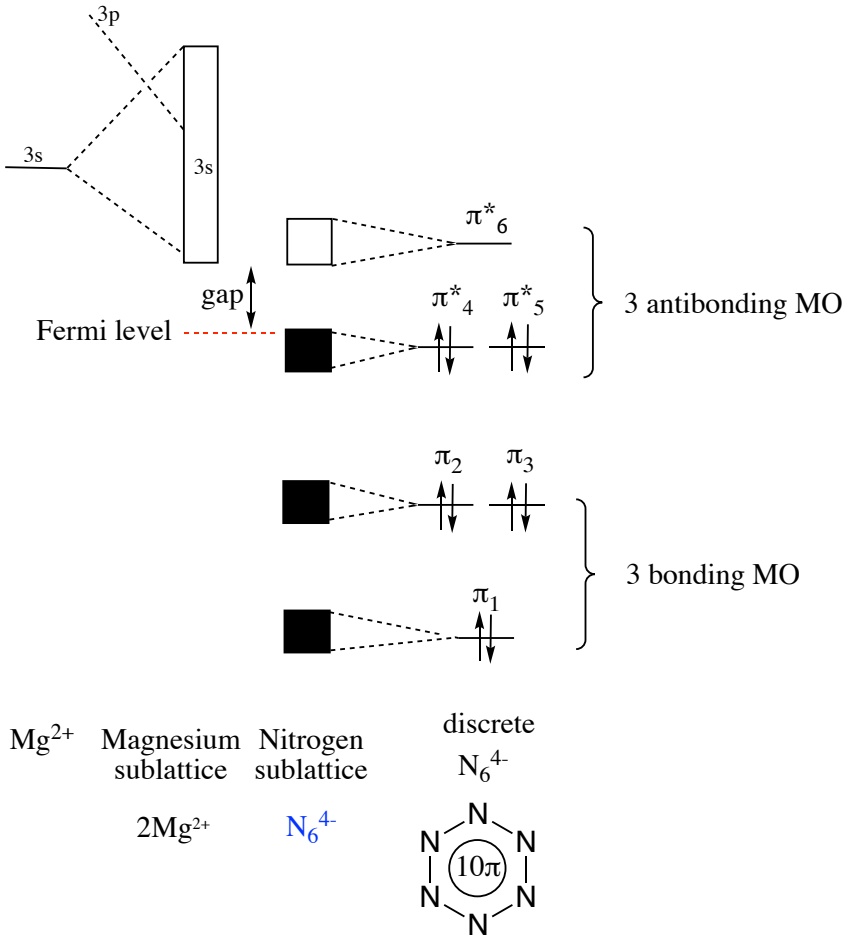

Figure S3 At right, molecular orbital levels of planar D_{6h} N_6^{4-} ring. Each level leads to localized π band (black boxes, occupied levels; empty boxes, unoccupied levels). At left, empty 3*s* level of Mg^{2+} atoms will lead to an empty 3*s* band. A band gap separates the valence and the conductions bands.

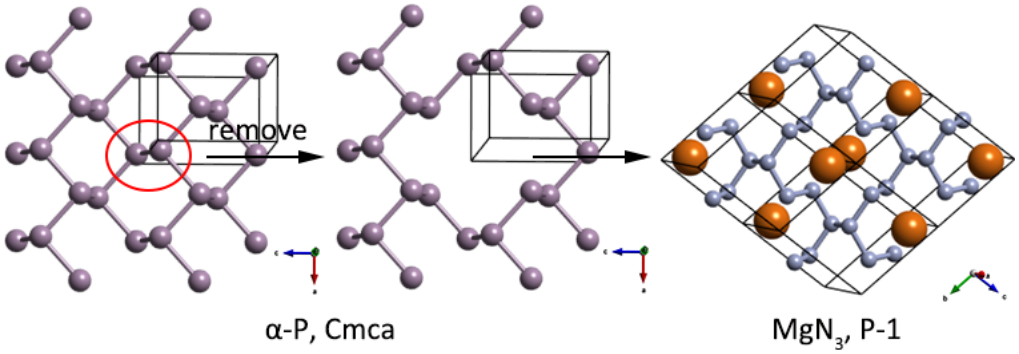

Figure S4 Structural relationship of α-P (*Cmca*) and MgN_3 (*P-1* (II)).

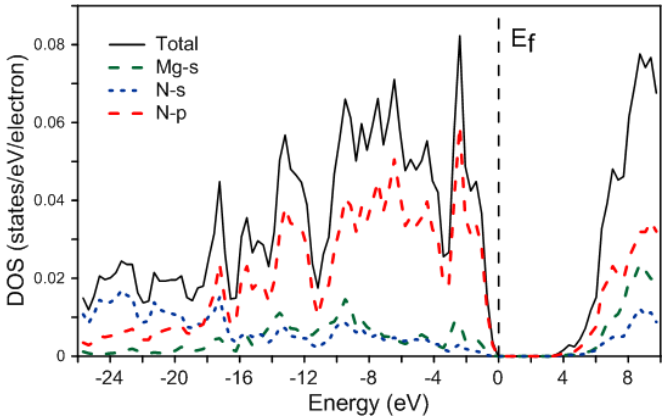

Figure S5 Calculated density of states (DOS) of *P-1* MgN_3 at 200 GPa at HSE06 hybrid functional level[28].

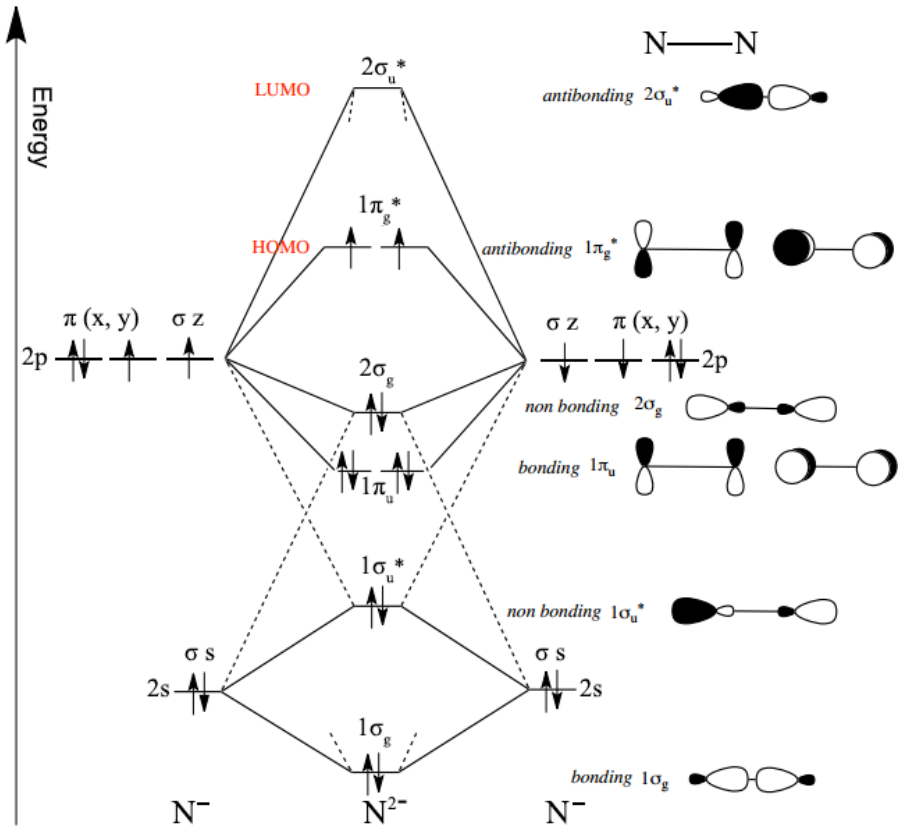

Figure S6 Molecular orbital diagram of diazenide N_2^{2-} unit in *Cmcm* MgN_2.

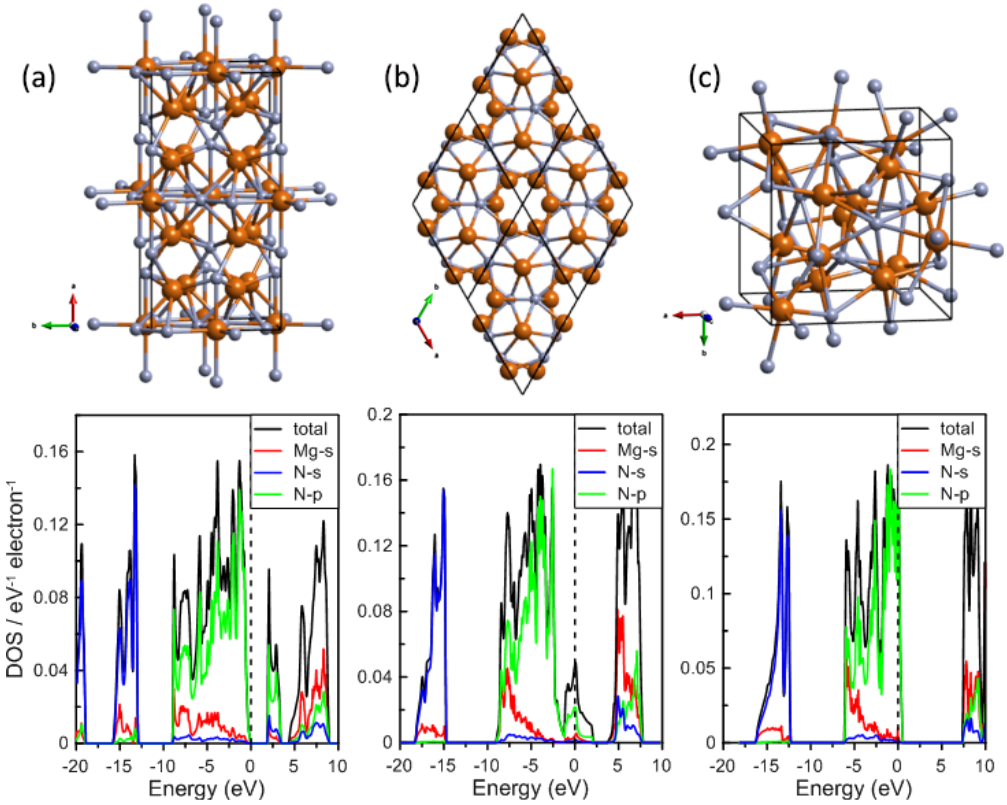

Figure S7 Crystal structures and electronic density of states of (a) *Cmca*-Mg_5N_4 at 100 GPa, (b) *P6₃/mcm*-Mg_5N_3 at 100 GPa and (c) *I-43d*-Mg_4N_3 at 100 GPa.

Table S4 Gravimetric energy densities for nitrogen-based materials and well-known explosives

A. Our results

Stoichiometry	Space group phase	Enthalpy (eV/atom)	Energy density[a]	
			(eV/f.u)	(kJ/g)
MgN_4	*P2/m*	-7.013	1.065	1.279
MgN_4	*P-1*	-6.879	1.735	2.084
MgN_4	*Cmmm*	-6.820	2.030	2.438
MgN_3	*C2/m*	-6.753	0.798	1.161
MgN_3	*P-1 (I)*	-6.459	1.974	2.872
MgN_2	*Cmcm*	-6.224	0.818	1.509
MgN_2	*$P6_3/mcm$*	-6.144	1.058	1.951
Mg_2N_3	*Pmmm*	-5.776	1.780	1.895
Mg_2N_3	*C2/m*	-6.023	0.545	0.580
Nitrogen	*Pa-3*	-8.320	-	-
Mg_3N_2	*Ia-3*	-5.038	-	-

[a]Energy density corresponds to the reaction enthalpy of $Mg_xN_y = x/3Mg_3N_2 + (3y-2x)/6N_2$, at ambient pressure (1 atm) and T=0 K. 1 eV = 96.487 kJ/mol, molecular mass: N=14.007 g/mol, Mg=24.305 g/mol

B. Published results

Compounds (space group)	Energy densities, in $kJ.g^{-1}$ (eV/f.u.)	References
MgN_4 (*P-1*)	2.01 (1.68)	Weil *et al.*[29]
	2.08 (1.74)[a]	*present work*
MgN_3 (*P-1*)	2.83 (1.97)	Weil *et al.*[29]
	2.87 (1.97)	*present work*
MgN_2(*$P6_3/mcm$*)	1.93 (1.05)	Weil *et al.*[29]
	1.95 (1.06)	*present work*
Mg_2N_3 (*Imm2*)	1.64 (1.79)[b]	Weil *et al.*[29]
(Pmmn)	*1.90 (1.78)*	*present work*
CrN_4	1.96	Kvashnin et al.[30]
$Pb(N_3)_2$	2.6	Agrawal et al.[31]
LiN_5	2.7	Peng et al.[29]
HfN_{10}	2.8	Zhang et al.[32]
N_2H	4.4	Yin et al.[33]
TiN_{10}	5.2	Zhang et al.[32]
TNT 2,4,6-trinitrotoluene	4.3	Agrawal et al.[31]
HMX $(CH_2)_4(NNO_2)_4$	5.7	Agrawal et al.[31]

[a] Our calculated results are given in italics for comparison.

[b] Their energy density values , 1.64 $kJ.g^{-1}$ = 1.79 eV/f.u., are not consistent.

Table S5 Chemical features of stable magnesium-nitrogen Mg_xN_y compounds from Wei et al results (0-100 GPa pressure range)[29].

Compounds[1]	Phases	Stability domain (GPa)	Structure type	Nitrogen net
MgN_4	*P-1* *Cmmm*	10~41 >41	1D armchair chains 2-coordinated N	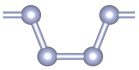
MgN_3	*P-1* (I)	>80	benzene-like N_6 rings	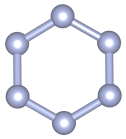
MgN_2	*Cmcm*	5~40	N_2 dumbbells	
	P6₃/mcm	>40	$N(N)_3$ three-pointed stars	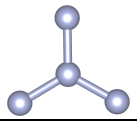
Mg_2N_3	*R-3m*[2]	5~37	Isolated nuclei + N_2 dumbbells	
	Imm2[2]	>37	bent N_3 units	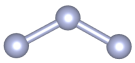
Mg_5N_7	***NO***			
Mg_5N_4	***NO***			
Mg_4N_3	***NO***			
MgN[3]	*P6₃/mmc*	*>80 GPa*	isolated nuclei	
Mg_3N_2	*Ia-3*	0~20	isolated nuclei	
	Pbcn	20~39	isolated nuclei	
	Pnma	>39	isolated nuclei	
Mg_5N_3	***NO***			

(1) CALYPSO crystal structure searches. PAW PBE DFT. [He]-core PAW potential for Mg and N.
(2) *R-3m* structure is similar to our *C2/m* structure. The difference comes from the tolerance factor used to symmetrize the DFT optimized structures.
(3) The published crystal structure *P6₃/mmc* MgN parameters in Table S1 of Wei et al.'s article leads to a Mg_3N_2 stoichiometry. Moreover, based on our calculations, MgN structures are metastable over the all pressure range of 0-300 GPa.
(4) The published crystal structure *P-1* MgN_4 parameters in Table S1 of Wei et al. shows different nitrogen network packing with snapshot in their manuscript.

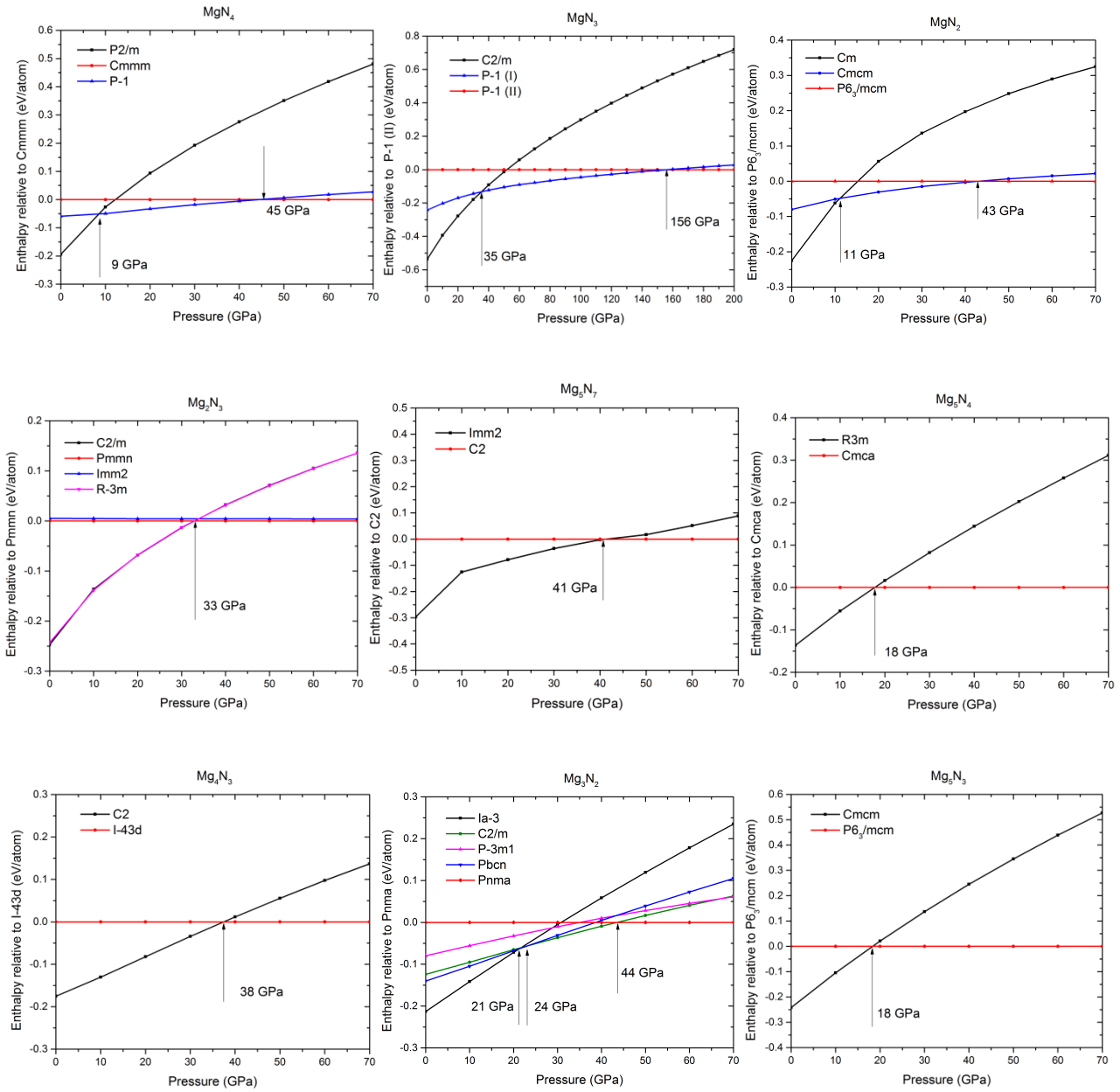

Figure S8 Relative enthalpies of various static ground state Mg_xN_y candidate structures* as a function of pressure. Plain red circles are the reference. Each phase transition is indicated by an arrow (Pressure in GPa). The DFT relaxed structure energy is calculated every 10 GPa from 0 GPa to 300 GPa. Structures of *P-1* MgN_4, *P-1* (I) MgN_3, *R-3m* and *Pmmn* Mg_2N_3, *Pnma* Mg_3N_2 phases are taken from the work of Wei *et al* (CALYPSO, 2017).[29] The *R-3m* and *Pmmn* Mg_2N_3 phases from CALYPSO results are nearly isoenergetic to our predicted USPEX *C2/m* and *Pmmn*.

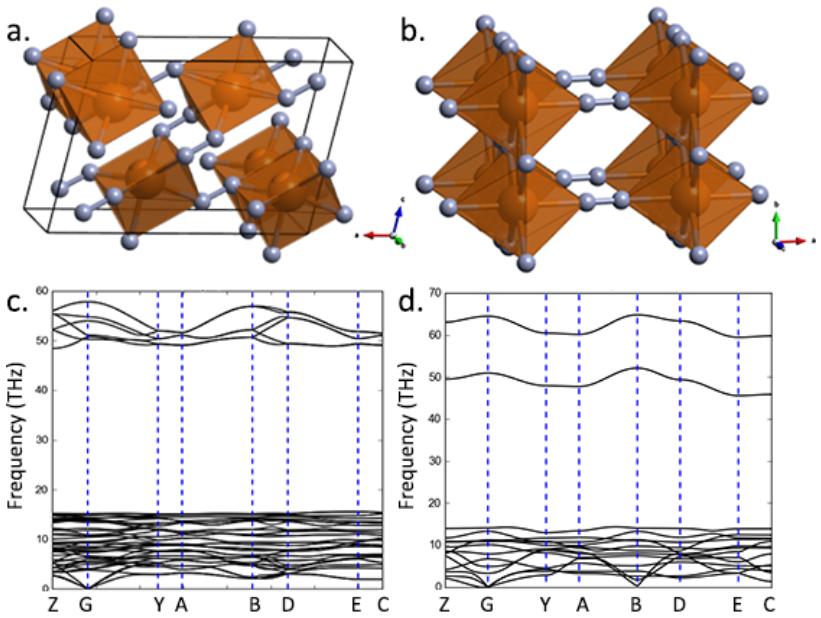

Figure S9 Crystal structures and phonon dispersion curves of *C2/m* MgN_3 at 0 GPa (a, c) and *P2/m* MgN_4 at 0 GPa (b, d).

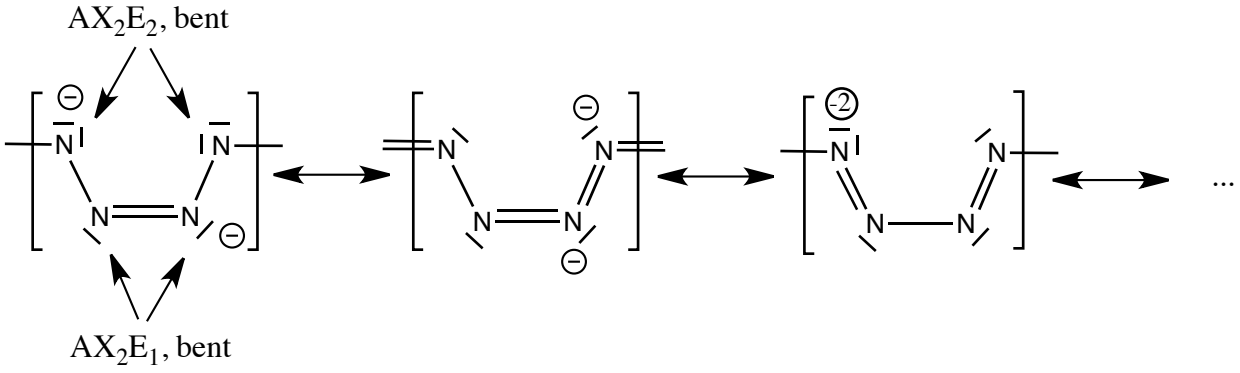

(a)

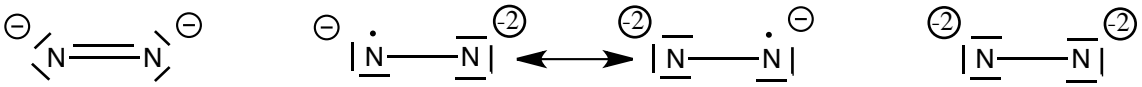

(b) (c) (d)

Figure S10 Lewis structures of (a) poly-N_4^{2-} (in *Cmmm* MgN_4), (b) N_2^{2-} (in *Cmcm* MgN_2, and *C2* Mg_5N_7), (c) N_2^{3-} (in *C2* Mg_5N_7), and (d) N_2^{4-} (in *Cmca* Mg_5N_4).

Ab initio molecular dynamics (AIMD) simulations: computational details and results

Ab initio (DFT) molecular dynamics simulations were performed with VASP for the case of a 3×2×4 (48 Mg and 192 N atoms; 240 atoms) *Cmmm* MgN_4-based periodic supercell. Starting from the *Cmmm* MgN_4 structure at ambient pressure, AIMD calculations were performed at 300 K, 600 K and 900 K. The timestep was 1 fs, and the total simulation time was as long as 10 ps. Brillouin zone integration was restricted to the Γ point of the supercell. A canonical NVT (N: constant number of particles, V: constant volume, and T: constant temperature) ensemble was adopted for the AIMD calculations using the algorithm of Nose, as implemented in the VASP code.

In our DFT calculations on Mg_xN_y phases, the PBE functional was used throughout this work. The projector-augmented wave (PAW) method was used for the core–electron representation. After preliminary convergence tests, we used a cutoff energy E_{cut}= 550 eV for the valence basis set.

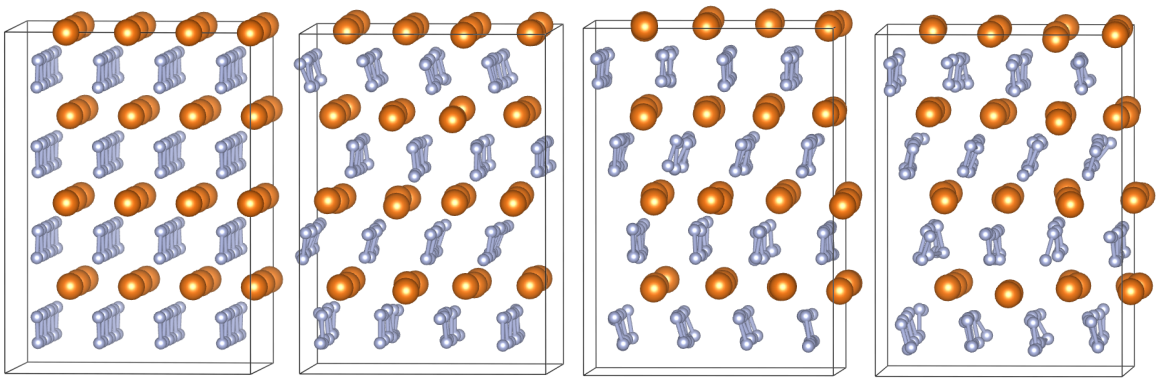

(a) (b) (c) (d)

Figure S11 Snapshots of the MgN_4 supercell at 1 atm (a) before AIMD (*Cmmm* phase at 0 K), and at the end of 10 ps AIMD simulations at (b) 300 K, (c) 600 K, and (d) 900 K. Small grey spheres are nitrogen atoms and large brown spheres are magnesium atoms.

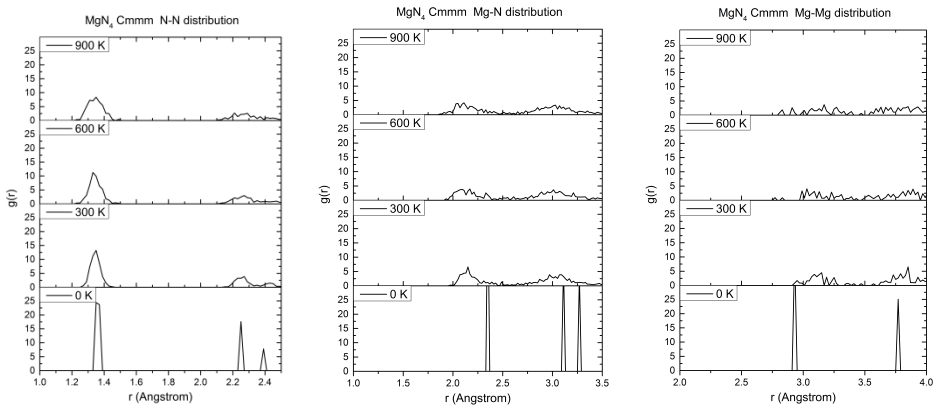

Figure S12 Radial distribution functions (RDF) for the (a) N-N, (b) Mg-N, and (c) Mg-Mg separations observed during AIMD simulations for *Cmmm* MgN_4-based supercell at ambient pressure and T = 0 K, 300 K, 600 K, and 900 K.

EHT calculations: computational details and results

All EHT calculations[29] were performed with the help of "Yet Another extended Hückel Molecular Orbital Package (YAeHMOP)". The standard atomic parameters were used for Mg and N (see Table below). The K-point sets for the average property (crystal orbital overlap population, COOP; density of states, DOS) calculations were chosen according to the literature. Crystalline structures are VASP optimized structures at a given pressure (see Table S1). Only COOP and DOS for *C*2 Mg_5N_7 (250 GPa) are given here to illustrate our EHT results for our chemical bonding analysis.

Atom	*Orbital*	H_{ii}, *eV*	ξ
Mg	*3s*	*-9.000*	*1.100*
	3p	*-4.500*	*1.100*
N	*2s*	*-26.000*	*1.950*
	2p	*-13.400*	*1.950*

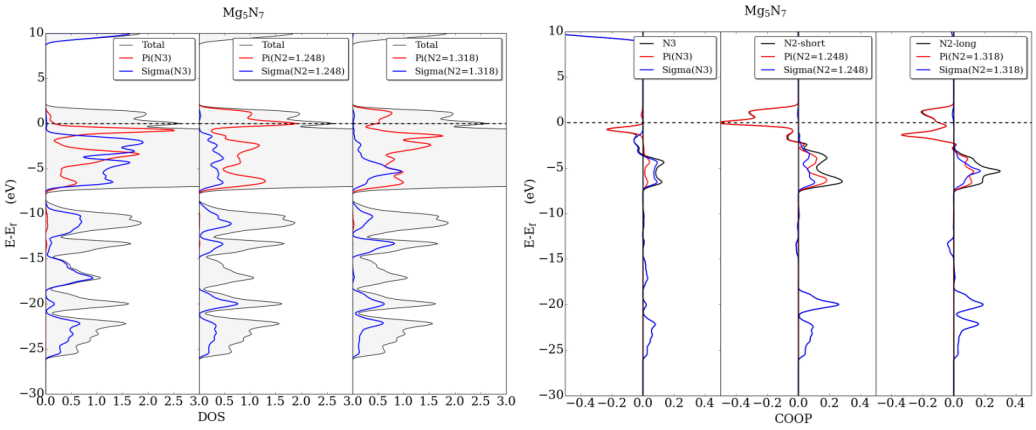

Figure S13 (a) Total and projected density of states (DOS), and (b) crystal orbital overlap population (COOP) of *C*2 Mg_5N_7 at 250 GPa.

Detonation properties: computational details

Velocity of detonation (VOD) and detonation pressure are two important performance parameters for energetic materials. The empirical Kamlet–Jacobs equations[32] were employed to estimate the values of detonation velocity (D) and detonation pressure (P) for *Cmmm* MgN_4 at 1 atm, as shown in the following equations:

$$D = 1.01(NM^{0.5}Q^{0.5})^{0.5}(1+1.30\rho)$$

$$P = 15.58\rho^2NM^{0.5}Q^{0.5}$$

where D is the detonation velocity (mm/μs = 10^{-6}km/10^{-6}s); P is the detonation pressure; N is the moles of gaseous detonation products, N_2(g), per gram of explosives (mol/g); M is the average molecular weights of gaseous products (g/mol); Q is the chemical energy of detonation (J/g) defined as the difference of the enthalpy of formation between products Mg_3N_2(s) and N_2(g), and reactant MgN_4(s), and ρ is the density of the explosive (g/cm^3). High explosives typically detonate at a rate between 5.5-9.5 km/s (velocity of detonation, VOD)

References

(1) Hao, J.; Li, Y.; Zhou, Q.; Liu, D.; Li, M.; Li, F.; Lei, W.; Chen, X.; Ma, Y.; Cui, Q. et al., Structural phase transformations of Mg_3N_2 at high pressure: experimental and theoretical studies. *Inorg. Chem.* **2009,** *48*, 9737-9741.

(2) Prasad, D. L. V. K.; Ashcroft, N. W.; Hoffmann, R., Evolving structural diversity and metallicity in compressed lithium azide. *JPCC* **2013,** *117*, 20838-20846.

(3) Shen, Y.; Oganov, A. R.; Qian, G.; Zhang, J.; Dong, H.; Zhu, Q.; Zhou, Z., Novel lithium-nitrogen compounds at ambient and high pressures. *Sci. Rep.* **2015,** *5*, 14204.

(4) Wang, X.; Li, J.; Botana, J.; Zhang, M.; Zhu, H.; Chen, L.; Liu, H.; Cui, T.; Miao, M., Polymerization of nitrogen in lithium azide. *J. Chem. Phys.* **2013,** *139*, 164710-164715.

(5) Steele, B. A.; Oleynik, I. I., Sodium pentazolate: A nitrogen rich high energy density material. *Chem. Phys. Lett.* **2015,** *643*, 21-26.

(6) Zhu, H. Y.; Zhang, F. X.; Ji, C.; Hou, D. B., Pressure-induced series of phase transitions in sodium azide. *J. Appl. Phys.* **2013,** *113*, 033511-033514.

(7) Zhang, J.; Zeng, Z.; Lin, H. Q.; Li, Y. L., Pressure-induced planar N_6 rings in potassium azide. *Sci. Rep.* **2014,** *4*, 4358.

(8) Li, J. F.; Wang, X. L.; Xu, N.; Li, D. Y.; Wang, D. C.; Chen, L., Pressure-induced polymerization of nitrogen in potassium azides. *Epl* **2013,** *104*, 236-247.

(9) Zhang, M. G.; Yan, H. Y.; Wei, Q.; Liu, H. Y., A new high-pressure polymeric nitrogen phase in potassium azide. *RSC Adv.* **2015,** *5*, 11825-11830.

(10) Wang, X. L.; Li, J. F.; Xu, N.; Zhu, H. Y.; Hu, Z. Y.; Li, C., Layered polymeric nitrogen in RbN_3 at high pressures. *Sci. Rep.* **2015,** *5*, 16677.

(11) Wang, X.; Li, J.; Zhu, H.; Chen, L.; Lin, H., Polymerization of nitrogen in cesium azide under modest pressure. *J. Chem. Phys.* **2014,** *141*, 044717.

(12) Feng, P.; Han, Y. X.; Liu, H. Y.; Yao, Y. S., Exotic stable cesium polynitrides at high pressure. *Sci. Rep.* **2015,** *5*, 16902.

(13) Zhu, S.; Peng, F.; Liu, H.; Majumdar, A.; Gao, T.; Yao, Y., Stable calcium nitrides at ambient and high pressures. *Inorg. Chem.* **2016,** *55*, 7550-7555.

(14) Zhang, X.; Zunger, A.; Trimarchi, G., Structure prediction and targeted synthesis: A new Na_nN_2 diazenide crystalline structure. *J. Chem. Phys.* **2010,** *133*, 194504.

(15) Babu, K. R.; Vaitheeswaran, G., Lattice dynamics and electronic structure of energetic solids LiN_3 and NaN_3: A first principles study. *Chem. Phys. Lett.* **2013,** *586*, 44-50.

(16) Zhang, M. G.; Yin, K.; Zhang, X. X.; Wang, H.; Li, Q.; Wu, Z. J.,*Structural and electronic properties of sodium azide at high pressure: A first principles study*. *Solid State Commun.* **2013,** *161*, 13-18.

(17) Zhu, H. Y.; Han, X.; Zhu, P. F.; Wu, X. X.; Chen, Y. M.; Li, M. R.; Li, X. F.; Cui, Q. L., The pressure-induced amorphization of strontium azide. *JPCC* **2016**, 12423-12428.

(18) Zhu, W.; Xu, X.; Xiao, H., Electronic structure and optical properties of crystalline strontium azide and barium azide by ab initio pseudopotential plane-wave calculations. *J. Phys. Chem. Solids* **2007,** *68*, 1762-1769.

(19) Vajenine, G. V.; Wang, X.; Efthimiopoulos, I.; Karmakar, S.; Syassen, K.; Hanfland, M., Structural phase transitions of sodium nitride at high pressure. *Phys. Rev. B: Condens. Matter* **2009,** *79*, 224107.

(20) Fischer, D.; Jansen, M., Synthesis and structure of K_3N. *Z. Anorg. Allg. Chem.* **2002,** *630*, 1755-1756.

(21) Xia, Y.; Li, Q.; Ma, Y. M., Novel superhard polymorphs of Be_3N_2 predicted by first-principles. *Comput. Mater. Sci.* **2010,** *49*, 76-79.

(22) Römer, S. R.; Dörfler, T.; Kroll, P.; Schnick, W., Group II element nitrides M_3N_2 under pressure: a comparative density functional study. *Physica Status Solidi* **2009,** *246*, 1604–1613.

(23) Vajenine, G. V., Plasma-assisted synthesis and properties of Na_3N. *Cheminform* **2007,** *38*, 5146-5148.

(24) Hao, J.; Li, Y.; Zhou, Q.; Liu, D.; Li, M.; Li, F.; Lei, W.; Chen, X.; Ma, Y.; Cui, Q., Structural phase transformations of Mg_3N_2 at high pressure: experimental and theoretical studies. *Inorg. Chem.* **2009,** *48*, 9737-9741.

(25) Braun, C.; Börger, S. L.; Boyko, T. D.; Miehe, G.; Ehrenberg, H.; Höhn, P.; Moewes, A.; Schnick, W., Ca_3N_2 and Mg_3N_2: unpredicted high-pressure behavior of binary nitrides. *JACS* **2011,** *133*, 4307-4315.

(26) Li, J.; Fan, C. Z.; Dong, X.; Jin, Y.; He, J. L., Theoretical investigation of the high-pressure structure, phase transition, and mechanical and electronic properties of Mg_3N_2. *JPCC* **2014,** *118*, 10238-10247.

(27) Dong, F. F.; Cheng, X. L.; Ge, S. H., Structural and electronic properties of $Sr(N_3)_2$ under pressure. *J. Theory Comput. Chem.* **2007,** *06*, 487-494.

(28) Paier, J.; Marsman, M.; Hummer, K.; Kresse, G.; Gerber, I. C.; Angyán, J. G., Screened hybrid density functionals applied to solids. *Journal of Chemical Physics* **2006,** *124*, 154709.

(29) Wei, S.; Li, D.; Liu, Z.; Li, X.; Tian, F.; Duan, D.; Liu, B.; Cui, T., Alkaline-earth metal (Mg) polynitrides at high pressure as possible high-energy materials. *PCCP* **2017,** *19*, 9246-9252.

(30) Kvashnin, A. G.; Oganov, A. R.; Samtsevich, A. I.; Allahyari, Z., Computational search for novel hard chromium-based materials. *Journal of Physical Chemistry Letters 8*, 755-764.

(31) Agrawal, J. P., *High Energy Materials: Propellants, Explosives and Pyrotechnics*. *Wiley: Weinheim* **2010**.

(32) Zhang, J.; Oganov, A. R.; Li, X.; Niu, H., Pressure-stabilized hafnium nitrides and their properties. *Physical Review B* **2017**, 020103.

(33) Yin, K.; Wang, Y.; Liu, H.; Peng, F.; Zhang, L.,*N_2H:* A novel polymeric hydronitrogen as a high energy density material. *Journal of Materials Chemistry A* **2015,** *3*, 4188-4194.